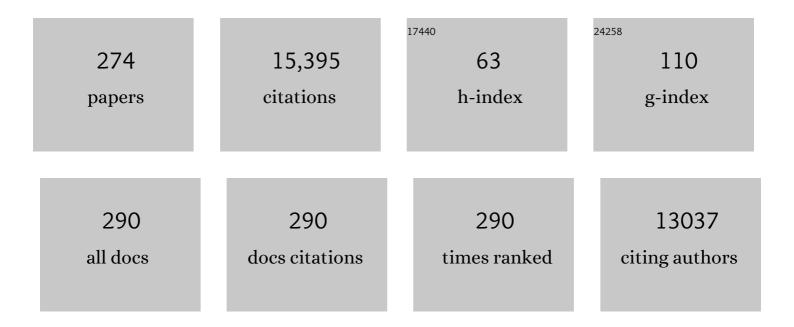
Linda J W Shimon

List of Publications by Year in descending order

Source: https://exaly.com/author-pdf/6157764/publications.pdf Version: 2024-02-01



#	Article	IF	CITATIONS
1	Efficient hydrogenation of organic carbonates, carbamates and formates indicates alternative routes to methanol based on CO2 and CO. Nature Chemistry, 2011, 3, 609-614.	13.6	563
2	Lowâ€Pressure Hydrogenation of Carbon Dioxide Catalyzed by an Iron Pincer Complex Exhibiting Noble Metal Activity. Angewandte Chemie - International Edition, 2011, 50, 9948-9952.	13.8	479
3	Consecutive Thermal H ₂ and Light-Induced O ₂ Evolution from Water Promoted by a Metal Complex. Science, 2009, 324, 74-77.	12.6	448
4	Manganese-Catalyzed Environmentally Benign Dehydrogenative Coupling of Alcohols and Amines to Form Aldimines and H ₂ : A Catalytic and Mechanistic Study. Journal of the American Chemical Society, 2016, 138, 4298-4301.	13.7	410
5	Direct Hydrogenation of Amides to Alcohols and Amines under Mild Conditions. Journal of the American Chemical Society, 2010, 132, 16756-16758.	13.7	394
6	Cellulosomes—Structure and Ultrastructure. Journal of Structural Biology, 1998, 124, 221-234.	2.8	306
7	Self-assembling dipeptide antibacterial nanostructures with membrane disrupting activity. Nature Communications, 2017, 8, 1365.	12.8	299
8	Electron-Rich, Bulky Ruthenium PNP-Type Complexes. Acceptorless Catalytic Alcohol Dehydrogenation. Organometallics, 2004, 23, 4026-4033.	2.3	285
9	Growth and Dissolution of Organic Crystals with ?Tailor-Made? Inhibitors?Implications in Stereochemistry and Materials Science. Angewandte Chemie International Edition in English, 1985, 24, 466-485.	4.4	271
10	Direct Conversion of Alcohols to Acetals and H ₂ Catalyzed by an Acridine-Based Ruthenium Pincer Complex. Journal of the American Chemical Society, 2009, 131, 3146-3147.	13.7	260
11	Metalâ^'Ligand Cooperation in Câ^'H and H2Activation by an Electron-Rich PNP Ir(I) System:Â Facile Ligand Dearomatizationâ^'Aromatization as Key Steps. Journal of the American Chemical Society, 2006, 128, 15390-15391.	13.7	222
12	Nâ^'H Activation of Amines and Ammonia by Ru via Metalâ^'Ligand Cooperation. Journal of the American Chemical Society, 2010, 132, 8542-8543.	13.7	214
13	Selective Bromination of Perylene Diimides under Mild Conditions. Journal of Organic Chemistry, 2007, 72, 5973-5979.	3.2	211
14	Manganeseâ€Catalyzed Hydrogenation of Esters to Alcohols. Chemistry - A European Journal, 2017, 23, 5934-5938.	3.3	192
15	Evidence for a terminal Pt(iv)-oxo complex exhibiting diverse reactivity. Nature, 2008, 455, 1093-1096.	27.8	187
16	Alkylâ^' and Arylâ^'Oxygen Bond Activation in Solution by Rhodium(I), Palladium(II), and Nickel(II). Transition-Metal-Based Selectivity. Journal of the American Chemical Society, 1998, 120, 6531-6541.	13.7	169
17	Cobalt atalyzed Hydrogenation of Esters to Alcohols: Unexpected Reactivity Trend Indicates Ester Enolate Intermediacy. Angewandte Chemie - International Edition, 2015, 54, 12357-12360.	13.8	166
18	Formation of η2 Câ^'H Agostic Rhodium Arene Complexes and Their Relevance to Electrophilic Bond Activation. Journal of the American Chemical Society, 1998, 120, 12539-12544.	13.7	164

#	Article	IF	CITATIONS
19	Electron-rich, bulky PNN-type ruthenium complexes: synthesis, characterization and catalysis of alcohol dehydrogenation. Dalton Transactions, 2007, , 107-113.	3.3	161
20	Reversible chromism of spiropyran in the cavity of a flexible coordination cage. Nature Communications, 2018, 9, 641.	12.8	148
21	Non-proteinaceous hydrolase comprised of a phenylalanine metallo-supramolecular amyloid-like structure. Nature Catalysis, 2019, 2, 977-985.	34.4	142
22	Light-emitting self-assembled peptide nucleic acids exhibit both stacking interactions and Watson–Crick base pairing. Nature Nanotechnology, 2015, 10, 353-360.	31.5	136
23	Rigid helical-like assemblies from a self-aggregating tripeptide. Nature Materials, 2019, 18, 503-509.	27.5	133
24	"Long-Range―Metalâ^'Ligand Cooperation in H ₂ Activation and Ammonia-Promoted Hydride Transfer with a Rutheniumâ^'Acridine Pincer Complex. Journal of the American Chemical Society, 2010, 132, 14763-14765.	13.7	129
25	Highly Efficient Process for Production of Biofuel from Ethanol Catalyzed by Ruthenium Pincer Complexes. Journal of the American Chemical Society, 2016, 138, 9077-9080.	13.7	128
26	A PCN Ligand System. Exclusive Câ^'C Activation with Rhodium(I) and Câ^'H Activation with Platinum(II). Organometallics, 1997, 16, 3981-3986.	2.3	127
27	Electrochromic Metallo-Organic Nanoscale Films: Fabrication, Color Range, and Devices. Journal of the American Chemical Society, 2017, 139, 11471-11481.	13.7	121
28	Synthesis, Structure, and Reactivity of New Rhodium and Iridium Complexes, Bearing a Highly Electron-Donating PNP System. Iridium-Mediated Vinylic Câ^'H Bond Activation. Organometallics, 2002, 21, 812-818.	2.3	120
29	A cohesin domain from Clostridium thermocellum: the crystal structure provides new insights into cellulosome assembly. Structure, 1997, 5, 381-390.	3.3	119
30	System with Potential Dual Modes of Metal–Ligand Cooperation: Highly Catalytically Active Pyridineâ€Based PNNH–Ru Pincer Complexes. Chemistry - A European Journal, 2014, 20, 15727-15731.	3.3	114
31	Selective Ortho Câ^'H Activation of Haloarenes by an Ir(I) System. Journal of the American Chemical Society, 2003, 125, 4714-4715.	13.7	111
32	Pincer "Hemilabile―Effect. PCN Platinum(II) Complexes with Different Amine "Arm Length― Organometallics, 2005, 24, 1082-1090.	2.3	111
33	Activation of Nitriles by Metal Ligand Cooperation. Reversible Formation of Ketimido- and Enamido-Rhenium PNP Pincer Complexes and Relevance to Catalytic Design. Journal of the American Chemical Society, 2013, 135, 17004-17018.	13.7	110
34	Reversible photoswitching of encapsulated azobenzenes in water. Proceedings of the National Academy of Sciences of the United States of America, 2018, 115, 9379-9384.	7.1	110
35	Rubrenes: Planar and Twisted. Chemistry - A European Journal, 2008, 14, 10639-10647.	3.3	109
36	Silanol-Based Pincer Pt(II) Complexes: Synthesis, Structure, and Unusual Reactivity. Inorganic Chemistry, 2008, 47, 7177-7189.	4.0	101

#	Article	IF	CITATIONS
37	orthoCâ^'H Activation of Haloarenes and Anisole by an Electron-Rich Iridium(I) Complex:Â Mechanism and Origin of Regio- andÂChemoselectivity. AnÂExperimental andÂTheoreticalÂStudy. Organometallics, 2006, 25, 3190-3210.	2.3	100
38	Controlling Rigidity and Planarity in Conjugated Polymers: Poly(3,4â€ethylenedithioselenophene). Angewandte Chemie - International Edition, 2009, 48, 5443-5447.	13.8	100
39	Unique Behavior of Dimethoxyethane (DME)/Mg(N(SO ₂ CF ₃) ₂) ₂ Solutions. Journal of Physical Chemistry C, 2016, 120, 19586-19594.	3.1	99
40	<i>Z</i> â€Selective (Crossâ€)Dimerization of Terminal Alkynes Catalyzed by an Iron Complex. Angewandte Chemie - International Edition, 2016, 55, 6942-6945.	13.8	98
41	Synthesis and Reactivity of an Iridium(I) Acetonyl PNP Complex. Experimental and Computational Study of Metalâ^'Ligand Cooperation in Hâ''H and Câ''H Bond Activation via Reversible Ligand Dearomatization. Organometallics, 2010, 29, 3817-3827.	2.3	97
42	Structural Analysis of Magnesium Chloride Complexes in Dimethoxyethane Solutions in the Context of Mg Batteries Research. Journal of Physical Chemistry C, 2017, 121, 24909-24918.	3.1	93
43	Crystallization of Organic Molecules: Nonclassical Mechanism Revealed by Direct Imaging. ACS Central Science, 2018, 4, 1031-1036.	11.3	88
44	Co-Crystallization of Sym-Triiodo-Trifluorobenzene with Bipyridyl Donors:Â Consistent Formation of Two Instead of Anticipated Three N··A·I Halogen Bonds. Crystal Growth and Design, 2007, 7, 386-392.	3.0	87
45	Self-Assembly of Aromatic Amino Acid Enantiomers into Supramolecular Materials of High Rigidity. ACS Nano, 2020, 14, 1694-1706.	14.6	86
46	Metal-Stabilized Methylene Arenium and σ-Arenium Compounds:  Synthesis, Structure, Reactivity, Charge Distribution, and Interconversion. Organometallics, 1999, 18, 895-905.	2.3	84
47	Formation of Stable <i>trans</i> -Dihydride Ruthenium(II) and 16-Electron Ruthenium(0) Complexes Based on Phosphinite PONOP Pincer Ligands. Reactivity toward Water and Electrophiles. Organometallics, 2009, 28, 4791-4806.	2.3	84
48	N–H Activation by Rh(I) via Metal–Ligand Cooperation. Organometallics, 2012, 31, 4083-4101.	2.3	83
49	Preparation and Characterization of New Ruthenium and Osmium Containing Polyoxometalates, [M(DMSO)3Mo7O24]4-(M = Ru(II), Os(II)), and Their Use as Catalysts for the Aerobic Oxidation of Alcohols. Inorganic Chemistry, 2003, 42, 3331-3339.	4.0	82
50	Exclusive Câ^'C Activation and an Apparent α-H Elimination with a Rhodium Phosphinite Pincer Complex. Organometallics, 2006, 25, 2292-2300.	2.3	82
51	Bioinspired Stable and Photoluminescent Assemblies for Power Generation. Advanced Materials, 2019, 31, e1807481.	21.0	82
52	Iron(II) complexes based on electron-rich, bulky PNN- and PNP-type ligands. Inorganica Chimica Acta, 2006, 359, 1955-1960.	2.4	79
53	Anionic Nickel(II) Complexes with Doubly Deprotonated PNP Pincer-Type Ligands and Their Reactivity toward CO ₂ . Organometallics, 2013, 32, 300-308.	2.3	79
54	Cationic, Neutral, and Anionic PNP Pd ^{II} and Pt ^{II} Complexes: Dearomatization by Deprotonation and Double-Deprotonation of Pincer Systems. Inorganic Chemistry, 2010, 49, 1615-1625.	4.0	78

#	Article	IF	CITATIONS
55	Oligofuran-containing molecules for organic electronics. Journal of Materials Chemistry C, 2013, 1, 4358.	5.5	77
56	How Innocent are Potentially Redox Non-Innocent Ligands? Electronic Structure and Metal Oxidation States in Iron-PNN Complexes as a Representative Case Study. Inorganic Chemistry, 2015, 54, 4909-4926.	4.0	76
57	Study of a bifuran vs. bithiophene unit for the rational design of π-conjugated systems. What have we learned?. Chemical Communications, 2013, 49, 6256.	4.1	71
58	Unsaturated Pd(0), Pd(I), and Pd(II) Complexes of a New Methoxy-Substituted Benzyl Phosphine. Arylâ^'X (X = Cl, I) Oxidative Addition, Câ^'O Cleavage, and Suzukiâ^'Miyaura Coupling of Aryl Chlorides. Organometallics, 2004, 23, 3931-3940.	2.3	70
59	Nickel promoted C–H, C–C and C–O bond activation in solution. Inorganica Chimica Acta, 2004, 357, 4015-4023.	2.4	70
60	Nucleophilic De-coordination and Electrophilic Regeneration of"Hemilabile―Pincer-Type Complexes: Formation of Anionic Dialkyl, Diaryl, and Dihydride PtII Complexes Bearing No Stabilizingi€-Acceptors. Chemistry - A European Journal, 2004, 10, 4673-4684.	3.3	69
61	Selfâ€Assembled Peptide Nanoâ€&uperstructure towards Enzyme Mimicking Hydrolysis. Angewandte Chemie - International Edition, 2021, 60, 17164-17170.	13.8	69
62	Molecular engineering of piezoelectricity in collagen-mimicking peptide assemblies. Nature Communications, 2021, 12, 2634.	12.8	68
63	Highly Coplanar Very Long Oligo(alkylfuran)s: A Conjugated System with Specific Head-To-Head Defect. Journal of the American Chemical Society, 2014, 136, 2592-2601.	13.7	67
64	Mononuclear Rh(II) PNP-Type Complexes. Structure and Reactivity. Inorganic Chemistry, 2007, 46, 10479-10490.	4.0	66
65	Single amino acid bionanozyme for environmental remediation. Nature Communications, 2022, 13, 1505.	12.8	66
66	Helically Locked Tethered Twistacenes. Journal of the American Chemical Society, 2018, 140, 8086-8090.	13.7	64
67	Photochemical Reduction of CO ₂ with Visible Light Using a Polyoxometalate as Photoreductant. Chemistry - A European Journal, 2017, 23, 92-95.	3.3	63
68	Directing Arylâ^'I versus Arylâ^'Br Bond Activation by Nickel via a Ring Walking Process. Inorganic Chemistry, 2008, 47, 5114-5121.	4.0	62
69	Spontaneous structural transition and crystal formation in minimal supramolecular polymer model. Science Advances, 2016, 2, e1500827.	10.3	62
70	Stable and optoelectronic dipeptide assemblies for power harvesting. Materials Today, 2019, 30, 10-16.	14.2	62
71	Redox-Induced Collapse and Regeneration of a Pincer-Type Complex Framework: A Nonplanar Coordination Mode of Palladium(II). Angewandte Chemie - International Edition, 2005, 44, 1709-1711.	13.8	61
72	Palladium Complexes of Perylene Diimides:Â Strong Fluorescence Despite Direct Attachment of Late Transition Metals to Organic Dyes. Inorganic Chemistry, 2007, 46, 4790-4792.	4.0	61

#	Article	IF	CITATIONS
73	Tunable Mechanical and Optoelectronic Properties of Organic Cocrystals by Unexpected Stacking Transformation from H- to J- and X-Aggregation. ACS Nano, 2020, 14, 10704-10715.	14.6	61
74	CC versus CH Activation and versus Agostic CC Interaction Controlled by Electron Density at the Metal Center. Chemistry - A European Journal, 2003, 9, 4295-4300.	3.3	60
75	Platinum Stilbazoles:Â Ring-Walking Coupled with Arylâ^'Halide Bond Activation. Journal of the American Chemical Society, 2005, 127, 9322-9323.	13.7	60
76	Diphenylalanine-Derivative Peptide Assemblies with Increased Aromaticity Exhibit Metal-like Rigidity and High Piezoelectricity. ACS Nano, 2020, 14, 7025-7037.	14.6	59
77	Synthesis and Structure of New Osmiumâ^'PCP Complexes. Osmium-Mediated Câ^'C Bond Activation. Organometallics, 2001, 20, 1719-1724.	2.3	57
78	C-Metalated Diazoalkane Complexes of Platinum Based on PCP- and PCN-Type Ligands. Organometallics, 2005, 24, 5937-5944.	2.3	57
79	Cationic, Neutral, and Anionic Platinum(II) Complexes Based on an Electron-Rich PNN Ligand. New Modes of Reactivity Based on Pincer Hemilability and Dearomatization. Organometallics, 2008, 27, 2627-2634.	2.3	57
80	Stepwise Assembly of Coordination-Based Metalâ^'Organic Networks. Journal of the American Chemical Society, 2010, 132, 14554-14561.	13.7	57
81	Modulating the Optical Properties of BODIPY Dyes by Noncovalent Dimerization within a Flexible Coordination Cage. Journal of the American Chemical Society, 2020, 142, 17721-17729.	13.7	57
82	Cobalt atalyzed Hydrogenation of Esters to Alcohols: Unexpected Reactivity Trend Indicates Ester Enolate Intermediacy. Angewandte Chemie, 2015, 127, 12534-12537.	2.0	56
83	Discovery of the First Metallaquinone. Journal of the American Chemical Society, 2000, 122, 8797-8798.	13.7	55
84	The Methylene-Transfer Reaction:Â Synthetic and Mechanistic Aspects of a Unique Câ^'C Coupling and Câ^'C Bond Activation Sequence. Journal of the American Chemical Society, 2000, 122, 7723-7734.	13.7	55
85	Two Structures of Alliinase from Alliium sativum L.: Apo Form and Ternary Complex with Aminoacrylate Reaction Intermediate Covalently Bound to the PLP Cofactor. Journal of Molecular Biology, 2007, 366, 611-625.	4.2	55
86	Synthesis, Structures, and Dearomatization by Deprotonation of Iron Complexes Featuring Bipyridine-based PNN Pincer Ligands. Inorganic Chemistry, 2013, 52, 9636-9649.	4.0	53
87	CO ₂ activation by manganese pincer complexes through different modes of metal–ligand cooperation. Dalton Transactions, 2019, 48, 14580-14584.	3.3	53
88	Methylene Arenium Cations via Quinone Methides and Xylylenes Stabilized by Metal Complexation. Journal of the American Chemical Society, 1998, 120, 477-483.	13.7	52
89	Structural Basis of Restoring Sequence-Specific DNA Binding and Transactivation to Mutant p53 by Suppressor Mutations. Journal of Molecular Biology, 2009, 385, 249-265.	4.2	52
90	CO Oxidation by N ₂ O Homogeneously Catalyzed by Ruthenium Hydride Pincer Complexes Indicating a New Mechanism. Journal of the American Chemical Society, 2018, 140, 7061-7064.	13.7	52

#	Article	IF	CITATIONS
91	Bâ^'C Bond Cleavage of BAr _F Anion Upon Oxidation of Rhodium(I) with AgBAr _F . Phosphinite Rhodium(I), Rhodium(II), and Rhodium(III) Pincer Complexes. Organometallics, 2008, 27, 2293-2299.	2.3	51
92	Long-Range Spin-Selective Transport in Chiral Metal–Organic Crystals with Temperature-Activated Magnetization. ACS Nano, 2020, 14, 16624-16633.	14.6	51
93	Oxidative Addition of Water to Novel Ir(I) Complexes Stabilized by Dimethyl Sulfoxide Ligands. Journal of the American Chemical Society, 2002, 124, 188-189.	13.7	49
94	Dimethylsulfoxide as a Ligand for RhI and Irl Complexes—Isolation, Structure, and Reactivity Towards XH Bonds (X=H, OH, OCH3). Chemistry - A European Journal, 2003, 9, 5237-5249.	3.3	49
95	sp3 C–H and sp2 C–H agostic ruthenium complexes: a combined experimental and theoretical study. Inorganica Chimica Acta, 2004, 357, 1854-1864.	2.4	49
96	Effect of CO on the Oxidative Addition of Arene CH Bonds by Cationic Rhodium Complexes. Chemistry - A European Journal, 2010, 16, 328-353.	3.3	49
97	Stepwise Metal–Ligand Cooperation by a Reversible Aromatization/Deconjugation Sequence in Ruthenium Complexes with a Tetradentate Phenanthrolineâ€Based Ligand. Chemistry - A European Journal, 2013, 19, 3407-3414.	3.3	49
98	Bottom-Up Construction of a CO2-Based Cycle for the Photocarbonylation of Benzene, Promoted by a Rhodium(I) Pincer Complex. Journal of the American Chemical Society, 2016, 138, 9941-9950.	13.7	49
99	A minimal length rigid helical peptide motif allows rational design of modular surfactants. Nature Communications, 2017, 8, 14018.	12.8	49
100	High-Efficiency Fluorescence through Bioinspired Supramolecular Self-Assembly. ACS Nano, 2020, 14, 2798-2807.	14.6	49
101	Guest Molecule-Mediated Energy Harvesting in a Conformationally Sensitive Peptide–Metal Organic Framework. Journal of the American Chemical Society, 2022, 144, 3468-3476.	13.7	49
102	Structure of a family IIIa scaffoldin CBD from the cellulosome ofClostridium cellulolyticumat 2.2â€Ã resolution. Acta Crystallographica Section D: Biological Crystallography, 2000, 56, 1560-1568.	2.5	48
103	DNA Recognition by the RUNX1 Transcription Factor Is Mediated by an Allosteric Transition in the RUNT Domain and by DNA Bending. Structure, 2002, 10, 1395-1407.	3.3	48
104	Rhodium complexes with chiral counterions: achiral catalysts in chiral matrices. Journal of Organometallic Chemistry, 2004, 689, 751-758.	1.8	48
105	Direct Observation of Reductive Elimination of MeX (X = Cl, Br, I) from Rh ^{III} Complexes: Mechanistic Insight and the Importance of Sterics. Journal of the American Chemical Society, 2013, 135, 11040-11047.	13.7	48
106	B–H Bond Cleavage via Metal–Ligand Cooperation by Dearomatized Ruthenium Pincer Complexes. Organometallics, 2014, 33, 3716-3726.	2.3	48
107	?-Accepting-Pincer Rhodium Complexes: An Unusual Coordination Mode of PCP-Type Systems. Chemistry - A European Journal, 2005, 11, 2319-2326.	3.3	47
108	Synthesis and Structure of Group 4 Symmetric Amidinate Complexes and Their Reactivity in the Polymerization of α-Olefins. Organometallics, 2013, 32, 6337-6352.	2.3	47

#	Article	IF	CITATIONS
109	A Stable "Endâ€On―Iron(III)–Hydroperoxo Complex in Water Derived from a Multiâ€Iron(II)â€Substituted Polyoxometalate and Molecular Oxygen. Angewandte Chemie - International Edition, 2008, 47, 9908-9912.	13.8	45
110	PNS-Type Ruthenium Pincer Complexes. Organometallics, 2012, 31, 6207-6214.	2.3	45
111	Coordination Chemistry of Nâ€Heterocyclic Nitreniumâ€Based Ligands. Chemistry - A European Journal, 2015, 21, 7099-7110.	3.3	45
112	Planar [6]Radialenes: Structure, Synthesis, and Aromaticity of Benzotriselenophene and Benzotrithiophene. Angewandte Chemie - International Edition, 2007, 46, 8814-8818.	13.8	44
113	Cation–cation bonding in nitrenium metal complexes. Chemical Science, 2014, 5, 1305.	7.4	44
114	Formation and X-ray Structures of PCP Ligand Based Platinum(II) and Palladium(II) Macrocycles. Inorganic Chemistry, 1996, 35, 7068-7073.	4.0	43
115	Competitive Câ^'I versus Câ^'CN Reductive Elimination from a Rh ^{III} Complex. Selectivity is Controlled by the Solvent. Journal of the American Chemical Society, 2008, 130, 14374-14375.	13.7	42
116	Metal–Ligand Cooperation Facilitates Bond Activation and Catalytic Hydrogenation with Zinc Pincer Complexes. Journal of the American Chemical Society, 2020, 142, 14513-14521.	13.7	41
117	Transition Metal-Catalyzed Silanone Generation. Journal of the American Chemical Society, 1996, 118, 10894-10895.	13.7	40
118	Solvent-Stabilized Alkylrhodium(III) Hydride Complexes: A Special Mode of Reversible Câ^'H Bond Elimination Involving an Agostic Intermediate. Chemistry - A European Journal, 2000, 6, 3287-3292.	3.3	40
119	PNN Ruthenium Pincer Complexes Based on Phosphinated 2,2′-Dipyridinemethane and 2,2′-Oxobispyridine. Metal–Ligand Cooperation in Cyclometalation and Catalysis. Organometallics, 2013, 32, 2973-2982.	2.3	40
120	Emergence of chirality and structural complexity in single crystals at the molecular and morphological levels. Nature Communications, 2020, 11, 380.	12.8	40
121	Novel Azine Reactivity: Facile NN Bond Cleavage, CH Activation, and NN Coupling Mediated by RhI. Angewandte Chemie - International Edition, 2003, 42, 1949-1952.	13.8	39
122	From Azobenzene Coordination to Arylâ^'Halide Bond Activation by Platinum. Organometallics, 2007, 26, 4528-4534.	2.3	39
123	Accelerated charge transfer in water-layered peptide assemblies. Energy and Environmental Science, 2020, 13, 96-101.	30.8	39
124	Atypical Cohesin-Dockerin Complex Responsible for Cell Surface Attachment of Cellulosomal Components. Journal of Biological Chemistry, 2013, 288, 16827-16838.	3.4	38
125	Stable Carbene and Diazoalkane Complexes of the Same Complex System. Synthesis, Structure, and Reactivity of PNPâ^'Ru(II) Fluorenylidene and Diazofluorene Complexes. Organometallics, 2008, 27, 3526-3533.	2.3	37
126	Osmium-Mediated CH and CC Bond Cleavage of a Phenolic Substrate:p-Quinone Methide and Methylene Arenium Pincer Complexes. Chemistry - A European Journal, 2007, 13, 1382-1393.	3.3	36

#	Article	IF	CITATIONS
127	Singlet fission in self-assembled PDI nanocrystals. Nanoscale, 2018, 10, 20147-20154.	5.6	36
128	Reactivity of Long Conjugated Systems: Selectivity of Diels–Alder Cycloaddition in Oligofurans. Organic Letters, 2012, 14, 502-505.	4.6	35
129	Precrystalline Aggregates Enable Control over Organic Crystallization in Solution. Angewandte Chemie - International Edition, 2016, 55, 179-182.	13.8	35
130	Consecutive Cyclometalation by Platinum(II). Organometallics, 1996, 15, 2562-2568.	2.3	34
131	2,4-Dimethoxy-2,4-dimethylpentan-3-one: An Aprotic Solvent Designed for Stability in Li–O2 Cells. Journal of the American Chemical Society, 2017, 139, 11690-11693.	13.7	34
132	Imidazole synthesis by transition metal free, base-mediated deaminative coupling of benzylamines and nitriles. Chemical Communications, 2017, 53, 13133-13136.	4.1	34
133	Chiral and SHG-Active Metal–Organic Frameworks Formed in Solution and on Surfaces: Uniformity, Morphology Control, Oriented Growth, and Postassembly Functionalization. Journal of the American Chemical Society, 2020, 142, 14210-14221.	13.7	34
134	Facile H/D Exchange at (Hetero)Aromatic Hydrocarbons Catalyzed by a Stable Trans-Dihydride N-Heterocyclic Carbene (NHC) Iron Complex. Journal of the American Chemical Society, 2020, 142, 17131-17139.	13.7	33
135	Inorganic–organic hybrid materials based on keggin type polyoxometalates and organic polyammonium cations. Journal of Molecular Structure, 2003, 656, 27-35.	3.6	32
136	Reactivity and stability of platinum(ii) formyl complexes based on PCP-type ligands. The significance of sterics. Dalton Transactions, 2007, , 5692.	3.3	32
137	Cocrystallization of a Tripyridyl Donor with Perfluorinated Iodobenzene Derivatives: Formation of Different NA·A·A·I Halogen Bonds Determining Network vs Plain Packing Crystals. Crystal Growth and Design, 2008, 8, 786-790.	3.0	31
138	Synthesis, Structure, and Reactivity of Nitrosyl Pincer-Type Rhodium Complexes. Organometallics, 2009, 28, 1917-1926.	2.3	31
139	New Tridentate Phosphine Rhodium and Iridium Complexes, Including a Stable Rhodium(I) Silyl. Siâ^'S Activation and a Strong Effect of X in (PP2)Mâ^'X (X = H, Cl, Me) on Siâ^'H Activation. Organometallics, 2002, 21, 5060-5065.	2.3	30
140	Pyridine-Based Sulfoxide Pincer Complexes of Rhodium and Iridium. Organometallics, 2008, 27, 1892-1901.	2.3	30
141	Dicobalt-μ-oxo Polyoxometalate Compound, [(α ₂ P ₂ W ₁₇ O ₆₁ Co) ₂ O] ^{14–} : A Potent Species for Water Oxidation, C–H Bond Activation, and Oxygen Transfer. Inorganic Chemistry, 2014. 53. 1779-1787.	4.0	30
142	Solid-State Crystal-to-Crystal Phase Transitions and Reversible Structure–Temperature Behavior of Phosphovanadomolybdic Acid, H ₅ PV ₂ Mo ₁₀ O ₄₀ . Inorganic Chemistry, 2015, 54, 628-634.	4.0	30
143	Reversible Aromaticity Transfer in a Bora-Cycle: Boron–Ligand Cooperation. Journal of the American Chemical Society, 2016, 138, 13307-13313.	13.7	30
144	Hydroboration of Nitriles, Esters, and Carbonates Catalyzed by Simple Earthâ€Abundant Metal Triflate Salts. Chemistry - an Asian Journal, 2021, 16, 999-1006.	3.3	30

#	Article	IF	CITATIONS
145	Structural variability in manganese(II) complexes of N,N′-bis(2-pyridinylmethylene) ethane (and propane) diamine ligands. Inorganica Chimica Acta, 2009, 362, 4713-4720.	2.4	29
146	Unsaturated Rh(I) and Rh(III) Naphthyl-Based PCP Complexes. Major Steric Effect on Reactivity. Organometallics, 2009, 28, 1900-1908.	2.3	29
147	Ru(0) and Ru(II) Nitrosyl Pincer Complexes: Structure, Reactivity, and Catalytic Activity. Inorganic Chemistry, 2013, 52, 11469-11479.	4.0	29
148	Reassembly and co-crystallization of a family 9 processive endoglucanase from its component parts: structural and functional significance of the intermodular linker. PeerJ, 2015, 3, e1126.	2.0	29
149	<i>Z</i> â€Selective (Crossâ€)Dimerization of Terminal Alkynes Catalyzed by an Iron Complex. Angewandte Chemie, 2016, 128, 7056-7059.	2.0	28
150	Bioinspired Flexible and Tough Layered Peptide Crystals. Advanced Materials, 2018, 30, 1704551.	21.0	28
151	Structure and Reactivity of Rhodium(I) Complexes Based on Electron-Withdrawing Pyrrolyl-PCP-Pincer Ligands. Organometallics, 2009, 28, 523-533.	2.3	27
152	Asymmetric Bis(formamidinate) Group 4 Complexes: Synthesis, Structure and Their Reactivity in the Polymerization of α-Olefins Organometallics, 2014, 33, 3119-3136.	2.3	27
153	Formation of bacterial pilus-like nanofibres by designed minimalistic self-assembling peptides. Nature Communications, 2016, 7, 13482.	12.8	27
154	Molecular Engineering of Self-Assembling Diphenylalanine Analogues Results in the Formation of Distinctive Microstructures. Chemistry of Materials, 2016, 28, 4341-4348.	6.7	27
155	Maximizing Property Tuning of Phosphorus Corrole Photocatalysts through a Trifluoromethylation Approach. Inorganic Chemistry, 2019, 58, 6184-6198.	4.0	27
156	Thiolâ€disulfide organization in alliin lyase (alliinase) from garlic (<i>Allium sativum</i>). Protein Science, 2009, 18, 196-205.	7.6	26
157	Fine-structural variance of family 3 carbohydrate-binding modules as extracellular biomass-sensing components of <i>Clostridium thermocellum</i> anti-σ ^I factors. Acta Crystallographica Section D: Biological Crystallography, 2014, 70, 522-534.	2.5	26
158	Design concept for α-hydrogen-substituted nitroxides. Nature Communications, 2015, 6, 6070.	12.8	26
159	Directed Molecular Structure Variations of Three-Dimensional Halogen-Bonded Organic Frameworks (XBOFs). Crystal Growth and Design, 2018, 18, 1967-1977.	3.0	26
160	Naphthyl-Based PCP Platinum Complexes. Nucleophilic Activation of Coordinated CO and Synthesis of a Pt(II) Formyl Complex. Organometallics, 2007, 26, 2931-2936.	2.3	25
161	Halogen-Bonded Supramolecular Assemblies Based on Phenylethynyl Pyridine Derivatives: Driving Crystal Packing through Systematic Chemical Modifications. Crystal Growth and Design, 2008, 8, 3066-3072.	3.0	25
162	Finding the Perfect Match: Halogen vs Hydrogen Bonding. Crystal Growth and Design, 2015, 15, 4756-4759.	3.0	25

#	Article	IF	CITATIONS
163	Synthesis of Imidazolin-2-iminato Titanium Complexes Containing Aryloxo Ligands and Their Catalytic Performance in the Polymerization of α-Olefins. Organometallics, 2016, 35, 1125-1131.	2.3	25
164	Collagen-Inspired Helical Peptide Coassembly Forms a Rigid Hydrogel with Twisted Polyproline II Architecture. ACS Nano, 2020, 14, 9990-10000.	14.6	25
165	Modulation of physical properties of organic cocrystals by amino acid chirality. Materials Today, 2021, 42, 29-40.	14.2	25
166	A New Ligand System Based on a Bipyridine-Functionalized Calix[4]arene Backbone Leading to Mono- and Bimetallic Complexes. Inorganic Chemistry, 2003, 42, 3160-3167.	4.0	24
167	Modular Arrangement of a Cellulosomal Scaffoldin Subunit Revealed from the Crystal Structure of a Cohesin Dyad. Journal of Molecular Biology, 2010, 399, 294-305.	4.2	24
168	Positive shift in corrole redox potentials leveraged by modest β-CF3-substitution helps achieve efficient photocatalytic C–H bond functionalization by group 13 complexes. Dalton Transactions, 2019, 48, 12279-12286.	3.3	24
169	Mechanically rigid supramolecular assemblies formed from an Fmoc-guanine conjugated peptide nucleic acid. Nature Communications, 2019, 10, 5256.	12.8	24
170	Formation of Fluorinated Platinumâ^ Stilbazole Complexes:Â Arylâ^ Halide Oxidative Addition vs Ε2-Coordination of a Carbonâ^ Carbon Double Bond. Organometallics, 2006, 25, 3308-3310.	2.3	23
171	A Unique Family of Stable and Water-Soluble <i>S</i> -Nitrosothiol Complexes. Inorganic Chemistry, 2008, 47, 4723-4733.	4.0	23
172	Intermodular Linker Flexibility Revealed from Crystal Structures of Adjacent Cellulosomal Cohesins of Acetivibrio cellulolyticus. Journal of Molecular Biology, 2009, 391, 86-97.	4.2	23
173	Structure of a family 3a carbohydrate-binding module from the cellulosomal scaffoldin CipA of <i>Clostridium thermocellum</i> with flanking linkers: implications for cellulosome structure. Acta Crystallographica Section F: Structural Biology Communications, 2013, 69, 733-737.	0.7	23
174	Coâ€Assembly Induced Solidâ€State Stacking Transformation in Amino Acidâ€Based Crystals with Enhanced Physical Properties. Angewandte Chemie - International Edition, 2022, 61, .	13.8	23
175	Preliminary X-ray characterization and phasing of a type II cohesin domain from the cellulosome ofAcetivibrio cellulolyticus. Acta Crystallographica Section D: Biological Crystallography, 2003, 59, 1670-1673.	2.5	22
176	Sonochemical Reaction of [Fe(CO)5] with 1-Methylimidazole in An Ionic Liquid: Formation of [(1-Methylimidazole)6Fell](PF6)2. European Journal of Inorganic Chemistry, 2005, 2005, 522-528.	2.0	22
177	A macrocyclic oligofuran: synthesis, solid state structure and electronic properties. Chemical Science, 2019, 10, 8527-8532.	7.4	22
178	Transition of Metastable Cross-α Crystals into Cross-β Fibrils by β-Turn Flipping. Journal of the American Chemical Society, 2019, 141, 363-369.	13.7	22
179	Redox Noninnocent Nature of Acridine-Based Pincer Complexes of 3d Metals and C–C Bond Formation. Organometallics, 2020, 39, 279-285.	2.3	22
180	Homogeneous Reforming of Aqueous Ethylene Glycol to Glycolic Acid and Pure Hydrogen Catalyzed by Pincerâ€Ruthenium Complexes Capable of Metal–Ligand Cooperation. Chemistry - A European Journal, 2021, 27, 4715-4722.	3.3	22

#	Article	IF	CITATIONS
181	Regioselective Transformation of Long π onjugated Backbones: From Oligofurans to Oligoarenes. Angewandte Chemie - International Edition, 2017, 56, 13601-13605.	13.8	21
182	Metal-Coordination-Induced Fusion Creates Hollow Crystalline Molecular Superstructures. Journal of the American Chemical Society, 2018, 140, 9132-9139.	13.7	21
183	Design, synthesis and crystal structure of a multiple donor–acceptor halogen bonded stilbazole: assembly of unimolecular interconnected helices. CrystEngComm, 2007, 9, 538-540.	2.6	20
184	Methylene Transfer from SnMe Groups Mediated by a Rhodium(I) Pincer Complex: SnC, CC, and CH Bond Activation. Chemistry - A European Journal, 2007, 13, 7501-7509.	3.3	20
185	Pyridine-based SNS-iridium and -rhodium sulfide complexes, including d8–d8 metal–metal interactions in the solid state. Dalton Transactions, 2008, , 3226.	3.3	20
186	Solvent-Dependent Interconversions between RhI, RhII, and RhIII Complexes of an Aryl–Monophosphine Ligand. Chemistry - A European Journal, 2007, 13, 9043-9055.	3.3	19
187	Crystal Structure of an Uncommon Cellulosome-Related Protein Module from Ruminococcus flavefaciens That Resembles Papain-Like Cysteine Peptidases. PLoS ONE, 2013, 8, e56138.	2.5	19
188	Strong Electroâ€Optic Effect and Spontaneous Domain Formation in Selfâ€Assembled Peptide Structures. Advanced Science, 2017, 4, 1700052.	11.2	19
189	Iron-catalysed ring-opening metathesis polymerization of olefins and mechanistic studies. Nature Catalysis, 2022, 5, 494-502.	34.4	19
190	Structure of a family 3b′ carbohydrate-binding module from the Cel9V glycoside hydrolase from <i>Clostridium thermocellum</i> : structural diversity and implications for carbohydrate binding. Acta Crystallographica Section D: Biological Crystallography, 2010, 66, 33-43.	2.5	18
191	Scaffoldin-borne family 3b carbohydrate-binding module from the cellulosome of <i>Bacteroides cellulosolvens</i> : structural diversity and significance of calcium for carbohydrate binding. Acta Crystallographica Section D: Biological Crystallography, 2011, 67, 506-515.	2.5	18
192	Tandem pinacol coupling–rearrangement of aromatic aldehydes with hydrogen catalyzed by a combination of a platinum complex and a polyoxometalate. Chemical Communications, 2007, , 3957.	4.1	17
193	Thermal stabilization of the protozoan <i>Entamoeba histolytica</i> alcohol dehydrogenase by a single proline substitution. Proteins: Structure, Function and Bioinformatics, 2008, 72, 711-719.	2.6	17
194	Opal-like Multicolor Appearance of Self-Assembled Photonic Array. ACS Applied Materials & Interfaces, 2018, 10, 20783-20789.	8.0	17
195	Formation of Coordinated Nitrosamines by Reaction of K[IrCl5NO] with Primary Amines. Organometallics, 2005, 24, 4707-4709.	2.3	16
196	Cohesin diversity revealed by the crystal structure of the anchoring cohesin from <i>Ruminococcus flavefaciens</i> . Proteins: Structure, Function and Bioinformatics, 2009, 77, 699-709.	2.6	16
197	A single mutation reforms the binding activity of an adhesion-deficient family 3 carbohydrate-binding module. Acta Crystallographica Section D: Biological Crystallography, 2012, 68, 819-828.	2.5	16
198	Superstructured metallocorroles for electrochemical CO ₂ reduction. Chemical Communications, 2019, 55, 11912-11915.	4.1	16

#	Article	IF	CITATIONS
199	Molecular cannibalism: Sacrificial materials as precursors for hollow and multidomain single crystals. Nature Communications, 2021, 12, 957.	12.8	15
200	Ternary host-guest complexes with rapid exchange kinetics and photoswitchable fluorescence. CheM, 2022, 8, 2362-2379.	11.7	15
201	Self-Oxidation of a Phenolate Complex to a Bimetallic Stilbene Quinone. Angewandte Chemie - International Edition, 2004, 43, 5961-5963.	13.8	14
202	Electronic Perturbation in a Molecular Nanowire of [IrCl ₅ (NO)] ^{â^`} Units. Chemistry - A European Journal, 2007, 13, 8428-8436.	3.3	14
203	Standalone cohesin as a molecular shuttle in cellulosome assembly. FEBS Letters, 2015, 589, 1569-1576.	2.8	14
204	Synthesis and stability of cyclic α-hydrogen nitroxides. Organic and Biomolecular Chemistry, 2015, 13, 10726-10733.	2.8	14
205	Electron-rich siloxane–platinum complexes — Synthesis, structures, and reactivity. Canadian Journal of Chemistry, 2005, 83, 786-792.	1.1	13
206	Activation of Molecular Oxygen by a Dioxygenase Pathway by a Ruthenium Bis-bipyridine Compound with a Proximal Selenium Site. Journal of the American Chemical Society, 2010, 132, 517-523.	13.7	13
207	Structural diversity in manganese, iron and cobalt complexes of the ditopic 1,2-bis(2,2′-bipyridyl-6-yl)ethyne ligand and observation of epoxidation and catalase activity of manganese compounds. Dalton Transactions, 2010, 39, 7266.	3.3	13
208	Autocatalytic and oscillatory reaction networks that form guanidines and products of their cyclization. Nature Communications, 2021, 12, 2994.	12.8	13
209	Expression, purification and crystallization of a cohesin domain from the cellulosome of Clostridium thermocellum. Journal of Biotechnology, 1996, 51, 243-249.	3.8	12
210	Photolysis of 4,4â€~-Dithiodipyridine Producescyclo-Octasulfur Molecules: A Basis for Au/S8Microcrystalline Systems. Chemistry of Materials, 2004, 16, 3976-3979.	6.7	12
211	A Coordination Controlled Aryl–Halide Oxidative Addition to Platinum. Chemistry - A European Journal, 2009, 15, 10025-10028.	3.3	12
212	Selfâ€Assembled Peptide Nanoâ€Superstructure towards Enzyme Mimicking Hydrolysis. Angewandte Chemie, 2021, 133, 17301-17307.	2.0	12
213	The Impact of Weak Cĩ£¿Hâ‹â‹â‹Rh Interactions on the Structure and Reactivity of <i>trans</i> â€{Rh(CO) ₂ (phosphine) ₂] ⁺ : An Experimental and Theoretical Examination. Chemistry - A European Journal, 2008, 14, 8183-8194.	3.3	11
214	Fluxional Behavior of Platinum(0) Complexes: Intra vs Intermolecular Reaction Pathways. Inorganic Chemistry, 2008, 47, 3815-3822.	4.0	11
215	Structural and magnetic behavior of mono- and dinuclear nickel (II) complexes of N,N′-bis-(3,5-dipiperidin-1-yl-[2,4,6]triazin-1-yl)-pyridin-2-ylmethyl-ethane-1,2-diamine. Inorganica Chimica Acta, 2009, 362, 4760-4766.	2.4	11
216	Structure of CBM3b of the major cellulosomal scaffoldin subunit ScaA from <i>Acetivibrio cellulolyticus</i> . Acta Crystallographica Section F: Structural Biology Communications, 2012, 68, 8-13.	0.7	11

#	Article	IF	CITATIONS
217	Stabilization of unique valencies of cobalt, nickel and copper by complexation with the tridentate ligand 2-(2′-pyridyl)-8-hydroxyquinoline. Polyhedron, 2013, 64, 365-370.	2.2	11
218	<i>O</i> , <i>O</i> ′-Diester Methylenediphosphonotetrathioate: Synthesis, Characterization, and Potential Applications. Journal of Organic Chemistry, 2013, 78, 270-277.	3.2	11
219	Mechanistic Aspects of Aryl–Halide Oxidative Addition, Coordination Chemistry, and Ringâ€Walking by Palladium. Chemistry - A European Journal, 2015, 21, 16113-16125.	3.3	11
220	Photocatalytic Splitting of CS ₂ to S ₈ and a Carbon–Sulfur Polymer Catalyzed by a Bimetallic Ruthenium(II) Compound with a Tertiary Amine Binding Site: Toward Photocatalytic Splitting of CO ₂ ?. Inorganic Chemistry, 2011, 50, 11273-11275.	4.0	10
221	A Twoâ€Tailed Phosphopeptide Crystallizes to Form a Lamellar Structure. Angewandte Chemie - International Edition, 2017, 56, 3252-3255.	13.8	10
222	Sorting of Molecular Building Blocks from Solution to Surface. Journal of the American Chemical Society, 2018, 140, 8162-8171.	13.7	10
223	Solid-state packing dictates the unexpected solubility of aromatic peptides. Cell Reports Physical Science, 2021, 2, 100391.	5.6	10
224	Biochemical and Structural Properties of Chimeras Constructed by Exchange of Cofactor-Binding Domains in Alcohol Dehydrogenases from Thermophilic and Mesophilic Microorganisms. Biochemistry, 2010, 49, 1943-1953.	2.5	9
225	Formation of Alkanes by Aerobic Carbon–Carbon Bond Coupling Reactions Catalyzed by a Phosphovanadomolybdic Acid. ACS Catalysis, 2017, 7, 2725-2729.	11.2	9
226	Modification of a Single Atom Affects the Physical Properties of Double Fluorinated Fmoc-Phe Derivatives. International Journal of Molecular Sciences, 2021, 22, 9634.	4.1	9
227	Title is missing!. Angewandte Chemie, 2003, 115, 1993-1996.	2.0	8
228	Iridiumâ^' and Rhodiumâ^'Silanol Complexes:Â Synthesis and Reactivity. Organometallics, 2003, 22, 4020-4024.	2.3	8
229	Quinone Methide Generation Based on acis-(N,N) Platinum Complex. Organometallics, 2007, 26, 2178-2182.	2.3	8
230	Closed and open framework architectures in copper(II) complexes with triazine substituted N,N′-bis-pyridin-2-ylmethyl-ethane-1,2-diamine ligands. Journal of Molecular Structure, 2008, 891, 491-497.	3.6	8
231	Modular Molecular Nanoplastics. ACS Nano, 2019, 13, 11097-11106.	14.6	8
232	Unusual Surface Texture, Dimensions and Morphology Variations of Chiral and Single Crystals**. Angewandte Chemie - International Edition, 2021, 60, 18256-18264.	13.8	8
233	Directing the Morphology, Packing, and Properties of Chiral Metal–Organic Frameworks by Cation Exchange**. Angewandte Chemie - International Edition, 2022, 61, .	13.8	8
234	New Ligand Systems Incorporating Two and Three 4,4â€~-Bipyridine Units. Characterization of Bi- and Trimetallic Rhodium and Iridium Complexes. Inorganic Chemistry, 2004, 43, 7180-7186.	4.0	7

#	Article	IF	CITATIONS
235	Crystallization and preliminary diffraction studies of CBM3b of cellobiohydrolase 9A from <i>Clostridium thermocellum</i> . Acta Crystallographica Section F: Structural Biology Communications, 2007, 63, 1044-1047.	0.7	7
236	Bioinspired Suprahelical Frameworks as Scaffolds for Artificial Photosynthesis. ACS Applied Materials & Interfaces, 2020, 12, 45192-45201.	8.0	7
237	Ring Size Determines the Conformation, Global Aromaticity and Photophysical Properties of Macrocyclic Oligofurans. Chemistry - A European Journal, 2021, 27, 17794-17801.	3.3	7
238	Alliin lyase (alliinase) from garlic (Allium sativum): crystallization and preliminary X-ray characterization. Acta Crystallographica Section D: Biological Crystallography, 2002, 58, 1335-1337.	2.5	6
239	Structure of alcohol dehydrogenase fromEntamoeba histolytica. Acta Crystallographica Section D: Biological Crystallography, 2006, 62, 541-547.	2.5	6
240	Noncellulosomal cohesin from the hyperthermophilic archaeon <i>Archaeoglobus fulgidus</i> . Proteins: Structure, Function and Bioinformatics, 2011, 79, 50-60.	2.6	6
241	Preliminary X-ray characterization of a novel type of anchoring cohesin from the cellulosome of <i>Ruminococcus flavefaciens</i> . Acta Crystallographica Section F: Structural Biology Communications, 2008, 64, 77-80.	0.7	5
242	Long-Range Through-Bond Heteronuclear Communication in Platinum Complexes. Inorganic Chemistry, 2009, 48, 4021-4030.	4.0	5
243	Regioselective Transformation of Long π onjugated Backbones: From Oligofurans to Oligoarenes. Angewandte Chemie, 2017, 129, 13789-13793.	2.0	5
244	Coassembly of Complementary Peptide Nucleic Acid into Crystalline Structures by Microfluidics. Small Methods, 2019, 3, 1900179.	8.6	5
245	Functional Coiled-Coil-like Assembly by Knob-into-Hole Packing of Single Heptad Repeat. ACS Nano, 2019, 13, 12630-12637.	14.6	5
246	Perfluorophenylâ€Bifuran: A Stable and Fluorescent Material Exhibiting Mechanofluorochromic Behavior. Helvetica Chimica Acta, 2019, 102, e1900027.	1.6	5
247	Unusual Surface Texture, Dimensions and Morphology Variations of Chiral and Single Crystals**. Angewandte Chemie, 2021, 133, 18404-18412.	2.0	5
248	Coexistence of 1 : 1 and 2 : 1 inclusion complexes of indigo carmine. Chemical Communicatio 3461-3464.	ns, 2022, 4.1	58 ₅
249	Crystallization and preliminary X-ray analysis ofAcetivibrio cellulolyticuscellulosomal type II cohesin module: two versions having different linker lengths. Acta Crystallographica Section F: Structural Biology Communications, 2008, 64, 58-61.	0.7	4
250	Aliphatic and aromatic C–H activation of benzo[h]quinolines by Rh(I). Unique precursor dependent formation of mono-, di- and trinuclear complexes. Inorganica Chimica Acta, 2011, 369, 260-269.	2.4	4
251	Crystallization and preliminary X-ray characterization of a type III cohesin–dockerin complex from the cellulosome system of <i>Ruminococcus flavefaciens</i> . Acta Crystallographica Section F: Structural Biology Communications, 2012, 68, 1116-1119.	0.7	4
252	Hexagonal Supramolecular Assemblies Based on a Rull(DMSO)3- or OsII(DMSO)3-Capped {HW9O33} Isopolyanion with Potassium Cations as Linkers. European Journal of Inorganic Chemistry, 2013, 2013, 1649-1653.	2.0	4

#	Article	IF	CITATIONS
253	Structural and EPR/ENDOR/ESEEM spectroscopic investigations of a vanadomolybdate Keggin-type polyoxometalate in organic solvent. Inorganica Chimica Acta, 2006, 359, 3072-3078.	2.4	3
254	Structural characterization of a novel autonomous cohesin from <i>Ruminococcus flavefaciens</i> . Acta Crystallographica Section F, Structural Biology Communications, 2014, 70, 450-456.	0.8	3
255	Novel Cu(I)-Selective Chelators Based on a Bis(phosphorothioyl)amide Scaffold. Inorganic Chemistry, 2014, 53, 7901-7908.	4.0	3
256	Crystal structure of disodium 2-amino-6-oxo-6,7-dihydro-1 <i>H</i> -purine-1,7-diide heptahydrate. Acta Crystallographica Section E: Crystallographic Communications, 2015, 71, 281-283.	0.5	3
257	Aerobic oxygenation catalyzed by first row transition metal complexes coordinated by tetradentate mono-carbon bridged bis-phenanthroline ligands: intra- <i>versus</i> intermolecular carbon–hydrogen bond activation. Dalton Transactions, 2019, 48, 6396-6407.	3.3	3
258	Coâ€Assembly Induced Solidâ€State Stacking Transformation in Amino Acidâ€Based Crystals with Enhanced Physical Properties. Angewandte Chemie, 2022, 134, .	2.0	3
259	Directing the Morphology, Packing, and Properties of Chiral MetalOrganic Frameworks by Cation Exchange. Angewandte Chemie, 0, , .	2.0	3
260	Thermophilic alcohol dehydrogenase from the mesophileEntamoeba histolytica: crystallization and preliminary X-ray characterization. Acta Crystallographica Section D: Biological Crystallography, 2002, 58, 546-548.	2.5	2
261	Reversible Temperature Dependent Dimerization of Transition Metal Substituted Quasi Wells-Dawson Polyfluoroxometalates. European Journal of Inorganic Chemistry, 2019, 2019, 482-485.	2.0	2
262	A Nanoscopic View of Photoinduced Charge Transfer in Organic Nanocrystalline Heterojunctions. Journal of Physical Chemistry C, 2019, 123, 25031-25041.	3.1	2
263	Noncovalent Bonding Caught in Action: From Amorphous to Cocrystalline Molecular Thin Films. ACS Nano, 2021, 15, 14643-14652.	14.6	2
264	Pathway-Dependent Coordination Networks: Crystals versus Films. Journal of the American Chemical Society, 2021, 143, 16913-16918.	13.7	2
265	Atomic insight into short helical peptide comprised of consecutive multiple aromatic residues. Chemical Communications, 2022, 58, 6445-6448.	4.1	2
266	Crystallization and preliminary X-ray analysis of a cohesin-like module from AF2375 of the archaeon <i>Archaeoglobus fulgidus</i> . Acta Crystallographica Section F: Structural Biology Communications, 2009, 65, 275-278.	0.7	1
267	Aminomethylene-Phosphonate Analogue as a Cu(II) Chelator: Characterization and Application as an Inhibitor of Oxidation Induced by the Cu(II)–Prion Peptide Complex. Inorganic Chemistry, 2019, 58, 8995-9003.	4.0	1
268	Easier to Twist than Bend: The Scope of the Bridge Formation Approach to Naphthalenophane Synthesis. Organic Materials, 2020, 02, 323-329.	2.0	1
269	Preparation and Characterization of New Ruthenium and Osmium Containing Polyoxometalates, [M(DMSO)3Mo7O24]4- (M: Ru(II), Os(II)), and Their Use as Catalysts for the Aerobic Oxidation of Alcohols ChemInform, 2003, 34, no.	0.0	0
270	Felix Frolow (1947–2014). Acta Crystallographica Section F, Structural Biology Communications, 2014, 70, 1443-1444.	0.8	0

#	Article	IF	CITATIONS
271	Os(VI)O2/K Metal–Organic Frameworks: Infinite Chain, Grid, and Porous Networks. Crystal Growth and Design, 2014, 14, 2703-2708.	3.0	0
272	Coordination Chemistry of N-Heterocyclic Nitrenium-Based Ligands. Chemistry - A European Journal, 2015, 21, 6969-6969.	3.3	0
273	Novel crown-ether–methylenediphosphonotetrathioate hybrids as Zn(<scp>ii</scp>) chelators. Dalton Transactions, 2015, 44, 21073-21080.	3.3	0
	Hydrogenâ€Atom Transfer Oxidation with H ₂ O ₂ Catalyzed by		

274